New inhibitors of dihydroorotate dehydrogenase (DHODH) based on the 4-hydroxy-1,2,5-oxadiazol-3-yl (hydroxyfurazanyl) scaffold

New inhibitors of dihydroorotate dehydrogenase (DHODH) based on the 4-hydroxy-1,2,5-oxadiazol-3-yl (hydroxyfurazanyl) scaffold.

Marco L. Lolli, Marta Giorgis, Paolo Tosco, Antonio Foti, Roberta Fruttero, Alberto Gasco

Dipartimento di Scienza e Tecnologia del Farmaco, Università degli Studi di Torino, via Pietro Giuria 9, 10125 Torino, Italy.

Correspondence:

Corresponding author. Dipartimento di Scienza e Tecnologia del Farmaco, Università di Torino, Via Pietro Giuria 9, I-10125 Torino, Italy; Tel.: +390116707670, Fax: +390116707286, E-mail:

Keywords: hydroxyfurazan, dihydroorotate dehydrogenase inhibitors, leflunomide, brequinar.

Abstract

Based on some structural analogies with leflunomide and brequinar, two well-known inhibitors of dihydroorotate dehydrogenase (DHODH), a new series of products was designed, by joining the substituted biphenyl moiety through an amide bridge to the 4-hydroxy-1,2,5-oxadiazol-3-yl scaffold. The compounds were studied for their DHODH inhibitory activity on rat liver mitochondrial/microsomal membranes. The activity was found to be closely dependent on the substitution pattern at the biphenyl system. The most potent products were those bearing two or four fluorine atoms at the phenyl adjacent to the oxadiazole ring. A modeling study showed that these structures bind the enzyme in a brequinar-like fashion and that their greater potency may depend partly on enhanced interactions with the hydrophobic ubiquinone channel, and partly on the role of such substituents in stabilizing the putative bioactive conformation.

1. Introduction

One step in pyrimidine biosynthesis is conversion of L-dihydroorotate (DHO) to orotate (ORO), under action of the enzyme dihydroorotate dehydrogenase (DHODH, EC 1.3.99.11), which contains a flavine (FMN) as redox cofactor [1]. In this transformation, electrons resulting from DHO oxidation are transferred to ubiquinone, and finally to cytochrome *c* oxidase. Previous studies have shown that this enzyme possesses two distinct binding sites, respectively for DHO/ORO and ubiquinone. Oxidation of DHO to ORO is the rate-limiting step of the whole pyrimidine biosynthetic pathway. Inhibitors of DHODH display antiproliferative and immunomodulator activities, and have shown potential benefits for treating rheumatoid arthritis (RA) [2-5]. RA is a chronic inflammation characterized by painful joints and progression to irreversible joint damage [6]. It is currently regarded as an immunological process involving a variety of mediators [7, 8]. Treatment relies on the traditional non-steroidal anti-inflammatory drugs (NSAIDs) or selective

COX-2 inhibitors (Coxibs) [9]. While these drugs may provide symptomatic relief, they do not modify the course of the disease. The main shortcoming of NSAIDs is their marked gastrotoxicity, whereas Coxibs potentially increase the risk of heart attack and stroke [10, 11]. Generally, both drugs are used in combination with disease-modifying anti-rheumatic drugs (DMARDs) for the management of established rheumatoid arthritis. Methotrexate is the principal DMARD, but other drugs in use include sulphasalazine, penicillamine, hydroxychloroquine and chloroquine, gold salts, cyclosporine and glucocorticoids [9, 12]. Hepatotoxicity, blood discrasias, intestinal and lung diseases are serious adverse effects of these drugs. Recently, biological agents able to activate pro-resolving biochemical pathways have been introduced onto the market; these include inhibitors of tumor necrosis factor-α (TNF-α). These inhibitors are used when arthritis is uncontrolled and serious toxic effects have arisen with DMARDs [9]. Inhibitors of DHODH have also been considered for treating RA; leflunomide (**1**) and brequinar (BQN, **2**) are the two most important such drugs (Figure 1) [13, 14]. The former is an isoxazol derivative, which behaves as a prodrug: upon absorption, it is rapidly converted into its active metabolite A771726 (**3**), which was assigned the *Z*-configuration. The latter was developed for cancer therapy, but failed in clinical trials due to limited therapeutic windows [15]. The binding sites for both A771726 and BQN are located at the narrow end of the channel that ubiquinone uses to accomplish a redox reaction with $FMNH_2$. Several charged and polar side chains (Gln47, His56, Tyr356, Thr360, and Arg136) are present at this position. In the A771726 binding mode, the deprotonated enolic OH group interacts via hydrogen bonding with Tyr356, while the amide carbonyl is hydrogen bonded to Arg136 through a water molecule [16]. In BQN, the binding mode is quite different. Here, the carboxylate group forms a salt bridge with Arg136, and is hydrogen bonded to Gln47. In addition, the biphenyl moiety establishes a number of hydrophobic contacts with several lipophilic residues of the tunnel. In a development of our quest for drugs to use as anti-inflammatory agents [17-19] we recently explored the possibility of using the 1,2,5-oxadiazole ring (furazan) as a replacement for the isoxazole moiety present in **1** [20]. Similarly to isoxazole in **1**, the furazans we designed (general structure **4**) are also

easily opened under physiological conditions, to yield the related α-oximinoacetonitrile derivatives (cyano-oximes) **5 (**Figure 2a). These products proved to be very poor DHODH inhibitors, probably due to the unfavorable *E*-configuration of the oxime moiety generated upon ring opening, which prevents hydrogen bonding to Tyr356 [20]. Since the attempt to restore this interaction by oxidizing the oximes to nitroderivatives was only partially successful, we decided to pursue another strategy, consisted in replacing the unsubstituted furazan in **5** with a hydroxyfurazan ring (**7a**, Figure 2b). The latter moiety is stable under physiological conditions, and should provide the correct orientation for the deprotonated hydroxyl, in order to mimic the enolate group of A771726 and interact likewise with Tyr356. The activity of **7a**, the first hydroxyfurazan analogue of A771726 that was tested, was not of great interest (4.3 μM), but nonetheless played a key role in the further development of our project. When **7a** was docked *in silico* at the DHODH active site, a BQN-like pose was obtained with the deprotonated furazan hydroxyl facing Arg136 instead of Tyr356. This amounted to a 180° flip of the furazan ring with respect to our expectations. From this observation, the suggestion arose that the hydroxyfurazan scaffold might have the potential to bind to DHODH like brequinar itself, thanks to its known bioisosterism with the carboxylic group [21]. A number of biphenyl derivatives linked to pentatomic arene- and cyclopentenecarboxylic acids through an amide bond (**6**, Figure 2b) were recently proposed as potent DHODH inhibitors. These inhibitors were found, by X-ray crystallography, to assume different poses in the ubiquinone binding site of DHODH, in some cases similar to BQN, in some others to A771726 [22, 23]. This paper describes a series of hydroxyfurazans (scheme 1) which displays moderate-to-high DHODH inhibitory activity, largely depending on the substitution pattern at the biphenyl ring.

2. Chemistry

The synthetic pathway used to obtain the final products is very straightforward (Scheme 1). The benzyloxy-substituted 1,2,5-oxadiazolecarboxylic acid **8**, a product we have described

elsewhere (see Experimental) was transformed into the corresponding carbonyl chloride **9** by action of thionyl chloride. This intermediate was treated with the appropriately-substituted anilines **10a-n** in the presence of pyridine, to afford the related amides **11a-n**. The same products were also obtained by direct coupling of the acid **8** with the corresponding anilines using HBTU (2-(1*H*-benzotriazole-1-yl)-1,1,3,3-tetramethyluronium hexafluorophosphate) in DMF. The amides **11a-n,** upon hydrogenation on Pd/C in THF, yielded the expected final compounds **7a-n**.

3. Inhibition of DHODH

The final products **7a-n** were assessed for their DHODH inhibitory activity on rat liver mitochondrial/microsomal membranes. A procedure adapted from the literature was employed (see Experimental), in which oxidation of DHO to ORO is monitored by following the concomitant reduction of the chromophore 2,6-dichlorophenolindophenol (DCIP) [24]; A771726 and BQN were taken as references. The reduction of DCIP was detected by the decrease in absorbance at 650 nm. The initial rate of the enzymatic reaction in the presence (v) and in the absence (V) of inhibitor was measured, and the IC_{50} value was calculated from eq. 1:

$$v = V / (1 + [I] / IC_{50}) \qquad (1)$$

in which $[I]$ is the concentration of the inhibitor. The results are collected in Table 1.

4. Results and discussion

Analysis of Table 1 shows that compound **7b**, in which the biphenyl scaffold does not bear any substituent, displays its inhibitory potency in the micromolar range (IC_{50} = 11 μM). If the amide bridge is moved from position 1 to 3 of the biphenyl system, product **7c** is yielded, whose potency is about 4 times lower. Adding a CF_3 group (which is present in A771726) to **7b,** at either position

4’ (compound **7d**) or position 3’ (compound **7e)** of the biphenyl moiety, again decreases the potency, approximately by one quarter and by one half, respectively. Conversely, considerable modulation in the inhibitory activity occurs when fluoro substitution is performed on the biphenyl system. Fluorine is a lipophilic substituent of small size, endowed with high electronegativity; its presence may affect the binding affinity of a compound to its target protein in many ways [25, 26]. The introduction of two or four fluorine atoms on the phenyl ring adjacent to the oxadiazole enhances the inhibitory potency of compounds **7f** and **7g** about 12-fold and 166-fold that of the parent structure. In both **7f** and **7g,** the introduction of a CF_3 group at position 4 or 3 of the second phenyl ring (products **7h**, **7i**; **7l**, **7m**) decreases the inhibitory potency which, nevertheless, remains higher than that of **7b**. By contrast, the presence of a trifluoromethoxy group at position 3’ (**7n**) affords the most active compound of the series, whose potency is comparable to that of BQN. In an attempt to rationalize the activity profile across the series, a molecular modeling study was carried out. A conformational search using an implicit solvent model was carried out for each of the newly synthesized compounds. This was followed by refinement of the geometry of local minima, through a quantum-mechanical (QM) method. Subsequently, flexible docking of the compounds was accomplished in three different crystallographic structures recovered from the Protein Data Bank (see Experimental). The complexes of the rat enzyme with BQN (PDB ID 1UUO), of the human enzyme with a BQN analogue (PDB ID 1D3G), and finally of human DHODH with a biphenylaminocarbonyl derivative of cyclopentenecarboxylic acid (PDB ID 2BXV), were chosen. The rat isoform was included, to explore whether small inter-species difference may play a role, while the two human complexes were selected in order to ascertain whether differences in the conformation of the Arg136 side chain might affect the binding mode, as observed by Baumgartner and co-workers [23]. Our docking protocol almost perfectly reproduced the BQN experimental pose in 1UUO and 1D3G (RMSD, respectively). No significant differences were observed among the poses obtained on the three targets. In all cases the compounds were found to bind in a BQN-like fashion, namely with the deprotonated hydroxyfurazan moiety facing Arg136, thus effectively

mimicking the carboxyl group of BQN and related compounds (Figure 3), while the hydroxyfurazan was in no case found to interact with Tyr356 in a leflunomide-like fashion. In spite of the good qualitative agreement, the scoring function implemented in AutoDock (see Experimental) was not able to reproduce the experimentally-observed differences in inhibitory potency across compounds **7a**-**n**. However, when the binding pose of the furazan derivatives was compared with the QM-refined global minimum obtained from the implicit solvent conformational search, we found excellent agreement for the derivatives bearing fluorine atoms on the biphenyl system, especially with regard to the dihedral angle between the amide nitrogen and the benzene ring (107.1° in the docking pose, 113.6° in the global minimum for **7n**, Figure 4A). Conversely, for compounds lacking aromatic fluorine atoms, in solution the benzene ring lies in the same plane as the amide bond, while in the putative bioactive conformation the two moieties are tilted by about 100° (106.1° for **7d**, Figure 4B). Since such a conformation would not fit into the ubiquinone site due to steric hindrance, the non-fluorinated compounds necessarily suffer a conformational strain penalty, in their attempt to assume a pose compatible with the constraints imposed by the geometry of the enzyme cavity.

5. Conclusions.

This study shows that it is possible to obtain a new class of DHODH inhibitors by joining the 4-hydroxy-1,2,5-oxadiazol-3-yl scaffold to substituted biphenyl moieties through an amide bridge. SAR analyses show that the most active compounds bear two or four fluorine atoms at the phenyl adjacent to the hetero-ring. The introduction of the trifluoromethoxy group at the 3'-position of the distal phenyl of **7m** gives rise to **7n,** which is an inhibitor as potent as BQN. A molecular modeling study rationalizes the beneficial role of the fluorine substituents, showing that these groups enhance the interactions with the hydrophobic ubiquinone channel of the enzyme, and stabilize the putative bioactive conformation.

6. Experimental Part

6.1 Chemistry.

Melting points were determined on a Büchi 530 apparatus. The compounds were routinely checked by IR spectroscopy (Shimadzu, FT-IR 8101M) and mass spectrometry (Finnigan-Mat TSQ-700 spectrometer, 70 eV, direct inlet). ^{1}H and proton decoupled ^{13}C-NMR spectra were recorded on a Bruker AC-300 spectrometer. The following abbreviations are used: s, singlet; d, doublet; q, quartet; m, multiplet; Fz, furazan. Flash column chromatography was performed on silica gel (Merck Kiesekgel 60, 230-400 mesh ASTM) using the indicated eluents. Thin layer chromatography (TLC) was carried out on 5×20 cm plates with a layer thickness of 0.25 mm; when necessary, they were developed with iodine and $KMnO_4$. Anhydrous magnesium sulphate was used as drying agent for the organic extracts. Elemental analyses of the new compounds are within ±0.4% of the theoretical values. The moisture-sensitive reactions were carried out under dry N_2 or Ar. Tetrahydrofuran (THF) was distilled immediately before use from sodium and benzophenone under N_2. Compounds **8** [21], A771726 [27], BQN [28] and the biphenyl-substituted anilines [29] were synthesized as described in the literature.

*6.1.1. 4-Benzyloxy-1,2,5-oxadiazole-3-carbonyl chloride (**9**).*

A solution of ~~**9**~~ **8** (500 mg, 2.27 mmol) and a drop of DMF in freshly distilled thionyl chloride (15 mL,) were stirred at room temperature for 24 h. The solution was concentrated under reduced pressure then distilled under reduced pressure in a Kugelrohr apparatus ($2 \cdot 10^{-5}$ bar, external bath 110 °C) to afford to the pure title compound as a low-melting-point white solid, used in the next step without any further purification, or stored under inert atmosphere. Yield 87 %; ^{1}H-NMR ($CDCl_3$) δ 5.44 (*s*, 2H, -C*H*$_2$O-), 7.40–7.49 (*m*, 5H, aromatic protons).

6.1.2. General procedure for amide synthesis

*6.1.2.1. Method A (from **8**).*

To a stirred solution of **8** (1.~~0~~ mmol), kept under inert atmosphere, and the appropriate substituted aniline (1 mmol) in dry DMF (25 mL), HBTU (2 mmol) was added portionwise. The resulting suspension was stirred for 6 h then poured into chilled 2M HCl (20 mL). The mixture was extracted exhaustively with Et_2O, the collected organic layers were dried and concentrated under reduced pressure. The residue was purified by flash chromatography, obtaining the title compound. For details of purification of the crude product, see the specific method.

*6.1.2.2. Method B (from **9**).*

A solution of the appropriate aniline (0.67 mmol) and dry pyridine (2 eq) in dry CH_2Cl_2 (4 mL) was added to a solution of **9** (1.2 eq) in dry CH_2Cl_2 (4 mL). The mixture was stirred overnight under inert atmosphere, then diluted with CH_2Cl_2 (15 mL), washed with 1M HCl (10 mL), 1M NaOH (10 mL), brine (10 mL), dried and concentrated under reduced pressure. For details of purification of the crude product, see the specific method.

*6.1.2.~~1~~4. 4-Benzyloxy-N-[(1-trifluoromethyl)phenyl-4-yl]-1,2,5-oxadiazole-3-carboxamide (**11a**).*

Method A was followed; flash chromatography eluent: petroleum ether 40-60/ethyl acetate 6:4 v/v. The solid was triturated with hexane/isopropyl ether 2/8 v/v; yield 25%; white solid (m.p. 142.4-142.6 °C, from hexane/isopropyl ether 2/8 v/v); ^{1}H-NMR ($CDCl_3$) δ 5.57 (*s*, 2H, C*H*$_2$O), 7.42-7.53 (*m*, 9H, aromatic protons), 11.36 (*s*, 1H, N*H*); ^{13}C-NMR ($CDCl_3$) δ 75.6, 120.2, 124.3 (*q*, *C*F$_3$ $^1J_{CF}$ 271.7 Hz), 127.0 (*q*, *C*(3); $^3J_{CF}$ 3.8 Hz), 127.7 (*q*, *C*(4); $^2J_{CF}$ 32.9 Hz), 129.1, 129.3, 129.8, 134.3, 139.0-140.0 (*m*), 141.3, 154.2, 163.8; MS (CI) 364 (M+1).

*6.1.2.~~3~~4. 4-Benzyloxy-N-(biphenyl-4-yl)-1,2,5-oxadiazole-3-carboxamide (**11b**).*

Method A was followed. The solid was triturated with diethyl ether; yield 88%; white solid (m.p. 185.8-186.1 °C from diethyl ether); ^{1}H-NMR (DMSO) δ 5.48 (*s*, 1H, C*H*$_2$O), 7.35-7.82 (*m*, 14H, aromatic protons), 11.1 (*s*, 1H, N*H*); ^{13}C-NMR (DMSO-d_6) δ 74.1, 120.7, 126.4, 126.9, 127.7, 128.4, 128.4, 128.7, 128.7, 134.4, 136.8, 137.1, 139.8, 142.2, 154.0, 163.3; MS (CI) 372 (M+1).

*6.1.2.~~4~~5. 4-Benzyloxy-N-(biphenyl-2-yl)-1,2,5-oxadiazole-3-carboxamide (**11c**).*

The general procedure from the carboxylic acid was followed (method A). Yield 70%; white solid (m.p. 122.6 – 123.0 °C); ^{1}H-NMR ($CDCl_3$) δ 5.29 (*s*, 1H, -C*H*$_2$O-), 7.22 – 8.48 (*m*, 14H, aromatic protons), 8.51 (*brs*, 1H, -N*H*-); ^{13}C-NMR ($CDCl_3$) δ 74.8, 121.4, 125.4, 128.3, 128.5, 128.6, 128.7, 129.1, 129.2, 129.3, 130.4, 132.7, 133.6, 133.8, 137.4, 141.4, 153.4, 162.7; MS(CI) 372 (M+1).

Formattato: Tipo di carattere: Non Corsivo

*6.1.2.~~5~~6. 4-Benzyloxy-N-[4'-(trifluoromethyl)biphenyl-4-yl]-1,2,5-oxadiazole-3-carboxyamide (**11d**).*

Method A was followed. The solid was triturated with isopropyl ether/hexane 1:1 v/v; yield 71%; white solid (m.p. 186.2-186.6 °C, from isopropyl ether/hexane 1:1 v/v); ^{1}H-NMR (DMSO-d_6-$CDCl_3$) δ 5.52 (*s*, 2H, -C*H*$_2$O-), 7.43-7.76 (*m*, 11H, aromatic protons), 8.48 (*s*, 1H, -*NH*); ^{13}C-NMR (DMSO-$CDCl_3$) ~~NMR~~ δ 74.5, 121.1, 124.5 (*q*, *C*F$_3$; $^{1}J_{CF}$ 271.9 Hz), 128.5 (*q*, -*C*(3'); $^{3}J_{CF}$ 3.9 Hz), 128.5 (*q*, -*C*(4'); $^{2}J_{CF}$ 31.2 Hz), 127.2, 127.6, 128.7, 128.7, 129.1, 134.6, 135.4, 138.3, 142.4, 143.9 (*br*), 154.4, 163.6; MS (CI) 440 (M+1).

*6.1.2.~~6~~7. 4-Benzyloxy-N-[3'-(trifluoromethyl)biphenyl-4-yl]-1,2,5-oxadiazole-3-carboxyamide (**11e**).*

Method A was followed. Yield 19%; white solid (m.p. 117.0 – 117.3 °C, from diisopropyl ether); ^{1}H-NMR ($CDCl_3$) δ 5.50 (*s*, 2H, -C*H*$_2$O-), 7.41-7.81. (*m*, 13H, aromatic protons), 8.45 (*s*, 1H, N*H*); ^{13}C-NMR ($CDCl_3$) δ 75.1, 120.6, 123.6 (*q*, $^{3}J_{CF}$ 5.1 Hz), 124.0 (*q*, $^{3}J_{CF}$ 4.6 Hz) (*C*(4')/*C*(2')), 124.1

(*q*, $^{1}J_{CF}$ 273.8 Hz, *C*F_3), 127.9, 128.6, 128.9, 129.1, (*q*, *C*(3'), $^{2}J_{CF}$ 34.3 Hz), 129.3, 129.4, 130.1, 124.0, 136.5, 136.8, 140.9, 141.2, 153.6, 163.3; MS (CI) 440 $(M+1)^+$.

*6.1.2.~~7~~8. 4-Benzyloxy-N-[(3,5-difluoro)biphenyl-4-yl]-1,2,5-oxadiazole-3-carboxyamide (**11f**).*

Method B was followed. Yield 62%; white solid (m.p. 144.8-145.0 °C, from diisopropyl ether/EtOH 9:1 v/v); ^{1}H-NMR ($CDCl_3$) δ 5.50 (*s*, 2H, CH_2O), 7.20-7.55 (*m*, 12H, aromatic protons), 8.01 (*s*, 1H, N*H*); ^{13}C-NMR ($CDCl_3$) δ 75.0, 110.3-110.6 (*m*, *C*(3)), 110.8 (*t*, *C*(2), $^{2}J_{CF}$ 17.1 Hz), 126.9, 128.5, 128.7, 128.8, 129.1, 129.1, 133.9, 138.2 (*t*, *C*(1'), $^{4}J_{CF}$ 2.8 Hz), 142.6 (*t*, *C*(4), $^{3}J_{CF}$ 9.3 Hz), 140.5, 153.7, 157.8 (*dd*, *C*(1), $^{1}J_{CF}$ 251.8 Hz, $^{3}J_{CF}$ 5.3 Hz), 163.4; MS (CI) 408 $(M+1)^+$.

*6.1.2.~~8~~9. 4-Benzyloxy-N-[(2,3,5,6-tetrafluoro)biphenyl-4-yl)-1,2,5-oxadiazole-3-carboxyamide (**11g**).*

Method B was followed. Yield 55%; white solid (m.p. 180.6-181.0 °C, from diisopropyl ether/EtOH 9:1 v/v); ^{1}H-NMR ($CDCl_3$) δ 5.50 (*s*, 2H, CH_2O), 7.47-7.72 (*m*, 10H, aromatic protons), 8.44 (*s*, 1H, N*H*); ^{13}C-NMR ($CDCl_3$) δ 75.2, 109.6-151.2 (aromatic signals), 140.2, 153.6, 163.4; MS (CI) 444 (M+1).

*6.1.2.~~9~~10. 4-Benzyloxy-N-[(3,5-difluoro-3'-trifluoromethyl)biphenyl-4-yl]-1,2,5-oxadiazole-3-carboxyamide (**11h**).*

Method B was followed. Yield 60%; the crude solid was triturated with diisopropyl ether/hexane 1:1 v/v; white solid (m.p. 120.5-120.9 °C, from diisopropyl ether); ^{1}H-NMR ($CDCl_3$) δ 5.49 (*s*, 2H, CH_2O), 7.23-7.77. (*m*, 11H, aromatic protons), 8.04 (*s*, 2H, mobile protons); ^{13}C-NMR ($CDCl_3$) δ 75.0, 110.6-141.8/156.1-159.5 (aromatic signals), 123.9 (*q*, *C*F_3, $^{1}J_{CF}$ 272.5 Hz), 140.4, 153.7, 163.4; MS (CI) 476 $(M+1)^+$.

*6.1.2.~~10~~11. 4-Benzyloxy-N-[(3,5-difluoro-4'-trifluoromethyl)biphenyl-4-yl]-1,2,5-oxadiazole-3-carboxyamide (**11i**).*

Method B was followed.; Yield 59%; the crude solid was triturated with diisopropyl ether/hexane 1:1 v/v; white solid (m.p. 144.6-144.8 °C, from diisopropyl ether); ^{1}H-NMR ($CDCl_3$) δ 5.52 (*s*, 2H, C*H*$_2$O), 7.25-7.76 (*m*, 11H, aromatic protons), 8.03 (*s*, 1H, N*H*); ^{13}C-NMR ($CDCl_3$) δ 75.0, 123.9 (*q*, *C*F$_3$, $^{1}J_{CF}$ 272.1 Hz), 110.7-141.6/156.1-159.5 (aromatic signals), 140.4, 153.9, 163.4; MS (CI) 476 $(M+1)^+$.

*6.1.2.~~11~~12. 4-Benzyloxy-N-[(2,3,5,6-tetrafluoro-4'-trifluoromethyl)biphenyl-4-yl]-1,2,5-oxadiazole-3-carboxyamide (**11l**).*

Method B was followed. Yield 56%; the crude solid was triturated with isopropyl ether/hexane 1:1 v/v; white solid (m.p. 196.0-196.4 °C, from diisopropyl ether/isopropanol 10:1 v/v). ^{1}H-NMR ($CDCl_3$) δ 5.47 (*s*, 2H, C*H*$_2$O), 7.38-7.99 (*m*, 5H, aromatic protons), 11.28 (*s*, 1H, N*H*); ^{13}C-NMR ($CDCl_3$) δ 74.2, 115.4-145.4 (aromatic signals), 123.9 (*q*, *C*F$_3$, $^{1}J_{CF}$ 272.1 Hz), 140.9, 154.5, 163.5; MS (CI) 512 $(M+1)^+$.

*6.1.2.~~12~~13. 4-Benzyloxy-N-[(2,3,5,6-tetrafluoro-3'-trifluoromethyl)biphenyl-4-yl]-1,2,5-oxadiazole-3-carboxyamide (**11m**).*

Method B was followed. Yield 56%; the crude solid was triturated with isopropyl ether/hexane 1:1 v/v; white solid (m.p. 132.6-133.8 °C, from diisopropyl ether/isopropanol 10:1 v/v); ^{1}H-NMR ($CDCl_3$) δ 5.43 (*s*, 2H, C*H*$_2$O), 7.26-7.76 (*m*, 11H, aromatic protons), 8.18 (*s*, 1H, mobile protons); ^{13}C-NMR ($CDCl_3$) δ 75.2, 103.3-145.8 (aromatic signals), 123.7 (*q*, *C*F$_3$, $^{1}J_{CF}$ 272.6 Hz), 140.1, 140.1, 153.6, 163.4; MS (CI) 512 $(M+1)^+$.

*6.1.2.~~13~~14. 4-Benzyloxy-N-[(2,3,5,6-tetrafluoro-3'-trifluoromethoxy)biphenyl-4-yl]-1,2,5-oxadiazole-3-carboxyamide (**11n**).*

Method B was followed. Yield 60%; the crude solid was triturated with isopropyl ether/hexane 3:7 v/v; white solid (m.p. 129.1-129.6 °C, from diisopropyl ether/isopropanol 10:1 v/v); ^{1}H-NMR ($CDCl_3$) δ 5.51 (*s*, 2H, C*H*$_2$O), 7.33-7.58 (*m*, 9H, aromatic protons), 8.10 (*s*, 1H, mobile protons); ^{13}C-NMR ($CDCl_3$) δ 75.2, 109.6-149.4 (aromatic signals), 120.4 (*q*, *C*F_3, $^{1}J_{CF}$ 257.9 Hz), 140.1, 153.5, 163.4; MS (CI) 528 $(M+1)^+$.

*6.1.3. General hydrogenation procedure to obtain the final products **7a-n**.*

Pd/C (16 mg) was added to a solution of the appropriate benzyloxyfurazanamide (**11a-n**, 0.2 mmol) in dry THF (10 mL). The resulting mixture was vigorously stirred under hydrogen atmosphere for 15-60 minutes. The suspension was filtered on a Celite bed, washing exhaustively with diethyl ether. The collected organic layers were concentrated under reduced pressure to obtain the title compound. See the specific method for purification details.

*6.1.3.1~~2~~. 4-Hydroxy-N-(1-trifluoromethyl)phenyl-4-yl)-1,2,5-oxadiazole-3-carboxyamide (**7a**).*

Yield 95%; white solid (m.p. 158.7-159.5 °C, from toluene); ^{1}H-NMR (DMSO-d_6) δ 7.70-8.03 (*m*, 4H, aromatic protons), 8.57 (*br s*, 2H, mobile protons); ^{13}C-NMR (DMSO-d_6) δ 120.2, 124.0 (*q*, *C*F_3, $^{1}J_{CF}$ 271.7 Hz), 124.7 (*q*, *C*(4), $^{2}J_{CF}$ 31.9 Hz), 126.2 (*q*, *C*(3), $^{3}J_{CF}$ 3.8 Hz), 141.2-141.3 (*m*), 142.9, 155.4, 162.2; MS (CI) 274 (M+1); anal. ($C_{10}H_6F_3N_3O_3$) C, H, N.

*6.1.3.~~1~~2. 4-Hydroxy-N-(biphenyl-4-yl)-1,2,5-oxadiazole-3-carboxyamide (**7b**).*

Yield 38%; the crude solid was triturated in hexane/isopropyl ether 3:7 v/v (m.p. 185.8-186.1 °C, from ethanol); ^{1}H-NMR (DMSO-d_6) δ 7.33-7.83 (*m*, 9H, aromatic protons), 11.03 (*s*, 1H, N*H*);

^{13}C-NMR (DMSO) 120.4, 126.3, 127.0, 127.2, 128.8, 136.2, 137.1, 139.4, 143.2, 154.8, 162.1; MS (CI) 282 (M+1); ~~Anal~~anal. ($C_{15}H_{11}N_3O_3$ 0.3H_2O) C, H, N.

*6.1.3.~~2~~3. 4-Hydroxy-N-(biphenyl-2-yl)-1,2,5-oxadiazole-3-carboxyamide (**7c**).*

The general hydrogenation procedure was followed. Yield 68% (m.p. 138.1 – 138.5 °C; from trituration with diisopropyl ether); ^{1}H-NMR ($CDCl_3$) δ 7.30 – 8.34 (*m*, 9H, *aromatic proton*), 8.56 (*s*, 1H, -O*H*), 8.72 (*s*, 1H, -*NH*-); ^{13}C-NMR ($CDCl_3$) δ 121.5, 126.3, 128.7, 128.7, 129.1, 129.5, 130.6, 132.4, 133.3, 136.7, 137.9, 157.2, 163.7; MS (CI) 282 (M+1); ~~Anal~~anal. ($C_9H_7N_3O_2$) C, H, N.

*6.1.3.~~3~~4. 4-Hydroxy-N-[4'-(trifluoromethyl)biphenyl-4-yl]-1,2,5-oxadiazole-3-carboxyamide (**7d**).*

Yield 55%; white solid (m.p. 191.3 – 191.9 °C dec., from EtOH/water); ^{1}H-NMR (DMSO-d_6) δ 7.81-7.92 (m, 8H, aromatic protons), 11.10 (s, 1H, NH); ^{13}C-NMR (DMSO-d_6) δ 124.3 (*q*, *C*F_3, $^1J_{CF}$ 271.9 Hz), 127.5 (*q*, *C*(4'), $^2J_{CF}$ 31.9 Hz), 125.7 (*q*, *C*(3'), $^3J_{CF}$ 3.3 Hz), 127.0, 127.5, 134.5, 138.5, 143.3, 143.3-143.4 (*m*), 155.0, 162.2; MS (CI) 350 (M+1); anal. ($C_{16}H_{10}F_3N_3O_3 \cdot 1.17H_2O$) C, H, N.

Formattato: Tipo di carattere: Symbol

*6.1.3.~~4~~5. 4-Hydroxy-N-[3'-(trifluoromethyl)biphenyl-4-yl]-1,2,5-oxadiazole-3-carboxyamide (**7e**).*

Purification by flash chromatography (eluent: CH_2Cl_2/MeOH 8:2 v/v). Yield 33%; white solid (m.p. 202.5 °C dec; from hexane/isopropyl ether 1:1 v/v); ^{1}H-NMR (DMSO-d_6) δ 7.66-8.00 (*m*, 8H, aromatic protons), 12.48 (*br s*, 2H, mobile protons), ^{13}C-NMR (DMSO-d_6) δ 120.2, 122.6 (*q*, *C*(4'), $^3J_{CF}$ 3.8 Hz), 123.6 (*q*, *C*(2'), $^3J_{CF}$ 3.6 Hz), 124.2 (*q*, *C*F_3, $^1J_{CF}$ 272.5 Hz), 127.5, 129.7 (*q*, *C*(3'), $^2J_{CF}$ 31.5 Hz), 130.0, 130.3, 133.9, 138.2, 140.5, 142.9, 157.2, 167.8; MS (CI) 338 (loss of CF_3 fragment; M+1); anal. ($C_{16}H_{10}F_3N_3O_3$ 1.19H_2O); calc.: C, 50.11; H, 3.63; N, 10.96; found: C, 49.66; H, 2.91; N, 10.84. HPLC purity 99% (mobile phase: MeOH/water with 0.1% trifluoroacetic acid 65/35 v/v, t_R = 8.15 min).

*6.1.3.~~5~~6. 4-Hydroxy-N-[(3,5-difluoro)biphenyl-4-yl]-1,2,5-oxadiazole-3-carboxyamide (**7f**).*

Yield 65%; white solid (m.p. 169.8-170.1 °C, from EtOH /water 1:1 v/v); ^{1}H-NMR (DMSO-d_6) δ 7.42-7.80 (*m*, 7H, aromatic protons), 10.78 (*s*, 1H, -N*H*); ^{13}C-NMR (DMSO-d_6) δ 110.1-110.4 (*m*, *C*(3)), 112.1 (*t*, *C*(1), $^{2}J_{CF}$ 17.5 Hz), 127.1, 128.9, 129.5, 137.4 (*t*, *C*(1'), $^{4}J_{CF}$ 2.2 Hz), 141.4 (*t*, *C*(4), $^{3}J_{CF}$ 9.7 Hz), 142.4, 155.6, 158.2 (*dd*, *C*(2), $^{1}J_{CF}$ 249.1 Hz $^{3}J_{CF}$ 6.0 Hz), 162.5; MS (CI) 318 (M+1); anal. ($C_{15}H_9F_2N_3O_3$1.3H_2O); calc.: C, 52.80; H, 3.44; N, 12.31; found: C, 52.37; H, 2.79; N, 11.63; HPLC purity 100% (mobile phase: MeOH/water with 0.1% trifluoroacetic acid 65/35 v/v, t_R = 3.53 min).

*6.1.3.~~6~~7. 4-Hydroxy-N-[(2,3,5,6-(tetrafluoro)biphenyl-4-yl]-1,2,5-oxadiazole-3-carboxyamide (**7g**).*

Yield 80%; white solid (m.p. 247.1-247.8 °C, from EtOH/water 1:1 v/v); ^{1}H-NMR (DMSO-d_6) δ 7.55-7.58 (*m*, 5H, aromatic protons), 11.27 (*s*, 1H, N*H*); ^{13}C-NMR (DMSO-d_6) δ 114.5-140.7 (aromatic signals), 141.8, 155.3, 162.4; MS (CI) 354 (M+1); anal. ($C_{15}H_7F_4N_3O_3$) C, H, N.

*6.1.3.~~7~~8. 4-Hydroxy-N-[(3,5-difluoro-3'-trifluoromethyl)biphenyl-4-yl]-1,2,5-oxadiazole-3-carboxyamide (**7h**).*

Yield 78%; white solid (m.p. 110.6-111.1 °C, from EtOH/water 1:1 v/v); ^{1}H-NMR (DMSO-d_6) δ 7.71-8.14 (*m*, 6H, aromatic protons), 10.84 (*s*, 1H, mobile protons); ^{13}C-NMR (DMSO-d_6) δ 110.2-141.5/156.6-160.0 (aromatic signals), 124.4 (*q*, CF_3, $^{1}J_{CF}$ 272.6 Hz), 142.5, 155.7, 162.7; MS (CI) 386 (M+1); anal. ($C_{16}H_8F_5N_3O_3 \cdot H_2O$) C, H, N.

*6.1.3.~~8~~9. 4-Hydroxy-N-[(3,5-difluoro-4'-trifluoromethyl)biphenyl-4-yl]-1,2,5-oxadiazole-3-carboxyamide (**7i**).*

Yield 87%; white solid (m.p. 167.7-168.4°C, from EtOH/water 1:2 v/v); ^{1}H-NMR (DMSO-d_6) δ 7.65-8.04 (*m*, 6H, aromatic protons), 8.86 (*s*, 2H, mobile protons); ^{13}C-NMR (DMSO-d_6) δ 110.5.141.2/156.2-159.2 (aromatic signals), 124.1 (*q*, CF_3, $^{1}J_{CF}$ 272.1 Hz), 142.1, 155.3, 162.3; MS (CI) 386 (M+1); anal. ($C_{16}H_8F_5N_3O_3$) C, H, N.

*6.1.3.~~9~~10. 4-Hydroxy-N-[(2,3,5,6-tetrafluoro-4'-trifluoromethyl)biphenyl-4-yl]-1,2,5-oxadiazole-3-carboxyamide (**7l**).*

Yield 91%; white solid (m.p. 260.3–263.7 °C, from EtOH/water 1:1 v/v); ^{1}H-NMR (DMSO-d_6) δ 7.85 – 7.98 (*d*, 4H, *aromatic protons*), 11.40 (*s*, 1H, *mobile protons*); ^{13}C-NMR ($CDCl_3$) 109.1 – 145.0 (aromatic signals), 123.9 (q, -CF_3 $^{1}J_{CF}$ 272. 3 Hz), 144.0, 155.3, 162.4; MS (CI) 422 (M+1); Anal. ($C_{16}H_6F_7N_3O_3$) C, H, N.

*6.1.3.~~10~~11. 4-Hydroxy-N-[(2,3,5,6-tetrafluoro-3'-trifluoromethyl)biphenyl-4-yl]-1,2,5-oxadiazole-3-carboxyamide (**7m**).*

Yield 92%; white solid (m.p. 171.3-171.6 °C, from EtOH/water 1:1 v/v); ^{1}H-NMR (DMSO-d_6) δ 7.80-8.04 (*m*; 4H, aromatic protons), 8.04 (*s*, 1H, mobile protons); ^{13}C-NMR ($CDCl_3$) 115.2-147.5 (aromatic signals), 123.81 (*q*, *C*F_3 $^{1}J_{CF}$ 272.43 Hz), 141.8, 155.3, 162.6; MS (CI) 422 (M+1); anal. ($C_{16}H_6F_7N_3O_3$) C, H, N.

*6.1.3.~~11~~12. 4-Hydroxy-N-[(2,3,5,6-tetrafluoro-3'-trifluoromethoxy)biphenyl-4-yl]-1,2,5-oxadiazole-3-carboxyamide (**7n**).*

Yield 85%; white solid (m.p. 183.9-184.2 °C, from EtOH/water 1:2 v/v); ^{1}H-NMR (DMSO-d_6) δ 7.55-7.75 (*m*; 4H, aromatic protons), 11.32 (*s*, 1H, mobile protons); ^{13}C-NMR (DMSO-d_6) 109.1-148.3 (aromatic signals), 120.0 (*q*, -O*C*F_3 $^{1}J_{CF}$ 256.8 Hz), 141.8, 155.3, 162.4; MS (CI) 438 (M+1); anal. ($C_{16}H_6F_7N_3O_4$) C, H, N.

6.2 Inhibition of rat liver DHODH activity.

6.2.1. Preparation of rat liver membranes

Crude mitochondrial/microsomal membranes from livers of male Wistar rats (200-250 g) were prepared by homogenization and differential centrifugation. Homogenization buffer was 25 mM sodium phosphate, 250 mM sucrose and 0.3% v/v Protease Inhibitor Cocktail for use with mammalian cell and tissue extracts (SIGMA Catalog Number P8340) at pH 7.4. The homogenate (9 mL homogenization buffer/g wet tissue) was centrifuged at 470*g* for 10 min, the supernatant retained, and the pellets re-homogenized in buffer (4.5 mL/g wet tissue). This homogenate was centrifuged (470*g*, 10 min) and the supernatant was combined with that obtained earlier, and centrifuged (50000*g*, 60 min). The membranes were washed by resuspention in homogenization buffer plus 150 mM NaCl, 1 mM EDTA and 1 mM EGTA before final centrifugation (50000*g*, 60 min) and re-suspension in the homogenization buffer (2 mL/g wet tissue). All the above steps were performed at 4 °C and aliquots of the final membrane preparation were stored at -80 °C.

6.2.2. Dihydroorotate dehydrogenase assay [20]

Inhibition of rat liver DHODH activity by the compounds tested was assessed using a DCIP-linked assay. Membranes (0.8 mg protein mL^{-1}) were incubated at 37 °C in 50 mM Tris-HCl, 0.1% Triton X-100, 1 mM KCN, pH 8.0 with coenzyme Q_{10} (100 μM) and the tested compounds at different concentrations (final DMSO concentration 0.1% v/v). The reaction was initiated by addition of DHO (500 μM), and the reduction of DCIP (50 μM) was monitored through decrease in absorbance at 650 nm. The initial rate of the enzyme reaction, in the presence/absence of potential inhibitor, was measured in the first five minutes (ε = 10400 M^{-1} cm^{-1} in our experimental conditions) and a

IC_{50} value was calculated from eq. 1:

$v = V / (1 + [I] / IC_{50})$

in which $[I]$ is the inhibitor concentration.

The Michaelis-Menten constant (K_m) for DHO, determined by the usual procedure, was found to be 14.6 μM, in keeping with previous studies [24].

6.3~~.~~ Molecular modeling

The molecular models of compounds **7a-n** and orotate were built in their dissociated form using standard bond lengths and angles, with the MOE software suite [30]. Following geometry optimization, a Monte Carlo conformational search was carried out with the ConfSearch module implemented in MOE. All molecular mechanics computations were performed with the Merck Force Field (MMFF94s) using the GB/SA implicit solvent model. The local minima obtained from the conformational search were then refined by *ab initio* QM optimization (RHF/6-31+G(d) level of theory, C-PCM polarizable continuum solvent model [31] using GAMESS-US [32]. The experimental crystallographic structures of DHODH complexes were retrieved from the Protein Data Bank [33] (PDB IDs 1UUO, 1D3G and 2BXV). The coordinates of a small number of residues were not resolved in these structures; since they were verified not to belong to the active site, the C- and N- termini upstream and downstream of the missing loops were simply capped with *N*-methyl and acetyl groups, respectively. Missing hydrogens were added to the three enzymes in standard positions, then optimized with the SANDER module of the AMBER 10 software package [34], while keeping heavy atoms harmonically restrained to the initial crystallographic coordinates with a force constant of 1000 kcal mol^{-1} $Å^{-2}$. AMBER FF99 parameters and charges were assigned to protein atoms, GAFF parameters coupled with QM-fitted RESP charges [35] were used for the co-crystallized inhibitor and orotate, while values for the FMN cofactor were taken from the literature [36]. After removing the co-crystallized inhibitor, docking of compounds ~~8a~~7a-~~m~~ n was carried out

Commentato [f1]: questa parentesi non si chiude

using AutoDock 4.2 [37]. A grid with a 0.375 Å step size was centered on the co-crystallized inhibitor, which was then removed; energy grid maps were pre-computed with AutoGrid, then flexible docking was carried out with AutoDock. The target proteins were kept rigid, while ligands were left free to explore the conformational space inside the enzyme cavity; 200 separate docking simulations were run on each protein, using the Lamarckian genetic algorithm with default parameters.

7. Acknowledgments.

ChemComp is acknowledged for financial support to molecular modeling study.

8. References.

[1] Jones, M. E. Pyrimidine nucleotide biosynthesis in animals: genes, enzymes, and regulation of UMP biosynthesis. Ann. Rev. Biochem. 49 (1980) 253-279.

[2] Davis, J. P.; Cain, G. A.; Pitts, W. J.; Magolda, R. L.; Copeland, R. A. The immunosuppressive metabolite of leflunomide is a potent inhibitor of human dihydroorotate dehydrogenase. Biochemistry 35 (1996) 1270-1273.

[3] Herrmann, M. L.; Schleyerbach, R.; Kirschbaum, B. J. Leflunomide: an immunomodulatory drug for the treatment of rheumatoid arthritis and other autoimmune diseases. Immunopharmacology 47 (2000) 273-289.

[4] Li, E. K.; Tam, L.-S.; Tomlinson, B. Leflunomide in the treatment of rheumatoid arthritis. Clin. Ther. 26 (2004) 447-459.

[5] Pally, C.; Smith, D.; Jaffee, B.; Magolda, R.; Zehender, H.; Dorobek, B.; Donatsch, P.; Papageorgiou, C.; Schuurman, H. J. Side effects of brequinar and brequinar analogues, in combination with cyclosporine, in the rat. Toxicology 127 (1998) 207-222.

[6] Akil, M.; Amos, R. S. ABC of rheumatology - rheumatoid-arthritis .1. Clinical-features and diagnosis. Brit. Med. J. ~~BMJ~~ 310 (1995) 587-590.

[7] Gilroy, D. W.; Lawrence, T.; Perretti, M.; Rossi, A. G. Inflammatory resolution: New opportunities for drug discovery. Nat. Rev. Drug Discovery 3 (2004) 401-416.

[8] Serhan, C. N. A search for endogenous mechanisms of anti-inflammation uncovers novel chemical mediators: missing links to resolution. Histochem. Cell Biol. 122 (2004) 305-321.

[9] Scott, D. L.; Wolfe, F.; Huizinga, T. W. J. Rheumatoid arthritis. Lancet 376 (2010) 1094-1108.

[10] Schaffer, D.; Florin, T.; Eagle, C.; Marschner, I.; Singh, G.; Grobler, M.; Fenn, C.; Schou, M.; Curnow, K. M. Risk of serious NSAID-related gastrointestinal events during long-term exposure: a systematic review. Med. J. Australia 185 (2006) 501-506.

[11] Scott, P. A.; Kingsley, G. H.; Smith, C. M.; Choy, E. H.; Scott, D. L. Non-steroidal anti-inflammatory drugs and myocardial infarctions: comparative systematic review of evidence from observational studies and randomised controlled trials. Ann. Rheum. Dis. 66 (2007) 1296-1304.

[12] Akil, M.; Amos, R. S. ABC of rheumatology - rheumatoid-arthritis. 2. Treatment. Brit. Med. J. 310 (1995) 652-655.

[13] Silva, H. T.; Morris, R. E. Leflunomide and malononitrilamides. Am. J. Med. Sci. 313 (1997) 289-301.

[14] Chen, S.-F.; Perrella, F. W.; Behrens, D. L. Inhibition of dihydroorotate dehydrogenase activity by brequinar sodium. Cancer Res. 52 (1992) 3521-3527.

[15] Maroun, J., Ruckdeschel, J. Natale, R. Morgan, R. Dallaire, B. Sisk, R. Gyves, J. Multicenter phase II study of brequinar sodium in patients with advanced lung cancer Cancer Chemoth. Pharm. 32 (1993) 64-66.

[16] Liu, S. P.; Neidhardt, E. A.; Grossman, T. H.; Ocain, T.; Clardy, J. Structures of human dihydroorotate dehydrogenase in complex with antiproliferative agents. Struct. Fold. Des. 8 (2000) 25-33.

[17] Chegaev, K.; Lazzarato, L.; Tosco, P.; Cena, C.; Marini, E.; Rolando, B.; Carrupt, P. A.; Fruttero, R.; Gasco, A. NO-donor COX-2 inhibitors. New nitrooxy-substituted 1,5-diarylimidazoles endowed with COX-2 inhibitory and vasodilator properties. J. Med. Chem. 50 (2007) 1449-1457 and references therein reported.

[18] Boschi, D.; Cena, C.; Di Stilo, A.; Rolando, B.; Manzini, P.; Fruttero, R.; Gasco, A. Nitrooxymethyl-Substituted Analogues of Rofecoxib: Synthesis and Pharmacological Characterization. Chem. Biodivers. 7 (2010) 1173-1182, and references therein reported.

[19] Cena, C.; Tosco, P., Marini, E., Lazzarato, L.; Piccinini. M.; Ramondetti, C.; Lupino, E.; Fruttero, R.; Gasco, A. Nitrooxyacyl derivatives od salicylic acid are aspirin-like molecules that covalently inactivate cyclooxygenase-1. ChemMedChem 2011, EarlyView and references therein reported.

[20] Giorgis, M., Lolli, M.L., Rolando, B., Rao, A.; Tosco, P.; Chaurasia, S.; Marabello, D.; Fruttero, R.; Gasco, A. 1,2,5-Oxadiazole analogues of leflunomide and related compounds. Eur. J. Med. Chem. 46 (2011) 383-392.

[21] Lolli, M. L.; Giordano, C.; Pickering, D. S.; Rolando, B.; Hansen, K. B.; Foti, A.; Contreras-Sanz, A.; Amir, A.; Fruttero, R.; Gasco, A.; Nielsen, B.; Johansen, T. N. 4-Hydroxy-1,2,5-oxadiazol-3-yl Moiety as Bioisoster of the Carboxy Function. Synthesis, Ionization Constants, and Molecular Pharmacological Characterization at Ionotropic Glutamate Receptors of Compounds Related to Glutamate and Its Homologues. J. Med. Chem. 53 (2010) 4110-4118.

[22] Leban, J.; Saeb, W.; Garcia, G.; Baumgartner, R.; Kramer, B. Discovery of a novel series of DHODH inhibitors by a docking procedure and QSAR refinement. Bioorg. Med. Chem. Lett. 14 (2004) 55-58.

[23] Baumgartner, R.; Walloschek, M.; Kralik, M.; Gotschlich, A.; Tasler, S.; Mies, J.; Leban, J. Dual binding mode of a novel series of DHODH inhibitors. J. Med. Chem. 49 (2006) 1239-1247.

[24] Ullrich, A.; Knecht, W.; Fries, M.; Loffler, M. Recombinant expression of N-terminal truncated

mutants of the membrane bound mouse, rat and human flavoenzyme dihydroorotate dehydrogenase - A versatile tool to rate inhibitor effects? Eur. J. Biochem. 268 (2001) 1861-1868.

[25] Purser, S.; Moore, P. R.; Swallow, S.; Gouverneur, V. Fluorine in medicinal chemistry. Chem. Soc. Rev. 37 (2008) 320-330.

[26] Bohm, H. J.; Banner, D.; Bendels, S.; Kansy, M.; Kuhn, B.; Muller, K.; Obst-Sander, U.; Stahl, M. Fluorine in medicinal chemistry. ChemBioChem 5 (2004) 637-643.

Commentato [f2]: è giusto che abbia lo stesso titolo del ref. 25?

[27] A. Ramakrishnan, K. N. K. Gobind, S. Dnyaneshwar, Intl. Appl. No.: PCT/IN2006/000359.

[28] Ackerman, Intl. Appl. No.: EP 0 339 485 B1, European Patent Specification 1989.

[29] Parrish C.A., Adams N.D., Auger K.R., Burgess J.L., Carson J.D., Chaudari A.M., Copeland R.A., Diamond M.A., Donatelli C.A., Duffy K.J., Faucette L.F., Finer J.T., Huffman W.F., Hugger E.D., Jackson J.R., Knight S.D., Luo L., Moore M.L., Newlander K.A., Ridgers L.H., Sakowicz R., Shaw A.N., Sung C.-M. M., Sutton D., Wood K.W., Zhang S.-Y., Zimmerman M.N., Dhanak D.; Novel ATP-Competitive Kinesis Spindle Protein Inhibitors; J. Med. Chem. 50 (2007) 4939-4952.

[30] MOE version 2010.11, Chemical Computing Group Inc., Montreal, Quebec, Canada.

[31] Tomasi, J.; Mennucci, B.; Cammi, R. Quantum mechanical continuum solvation models. Chem. Rev. 105 (2005) 2999-3094.

[32] GAMESS-US version 25 March 2010, Iowa State University, Ames, IA; Schmidt, M. W.; Baldridge, K. K.; Boatz, J. A.; Elbert, S. T.; Gordon, M. S.; Jensen, J. H.; Koseki, S.; Matsunaga, N.; Nguyen, K. A.; Su, S. J.; Windus, T. L.; Dupuis, M.; Montgomery, J. A. General atomic and molecular electronic structure system. J. Comput. Chem. 14 (1993) 1347-1363

[33] The Protein Data Bank; http://www.rcsb.org/ (Accessed 6 June 2011).

[34] AMBER 10; Case, D. A.; Darden, T. A.; Cheatham, T. E. III; Simmerling, C.L.; Wang, J.; Duke, R.E.; Luo, R.; Crowley, M.; Walker, R. C.; Zhang, W.; Merz, K. M.; Wang, B.; Hayik,

S.; Roitberg, A.; Seabra, G.; Kolossvary, I.; Wong, K.F.; Paesani, F.; Vanicek, J.; Wu, X.; Brozell, S. R.; Steinbrecher, T.; Gohlke, H.; Yang, L.; Tan, C.; Mongan, J.; Hornak, V.; Cui, G.; Mathews, D. H.; Seetin, M.G.; Sagui, C.; Babin, V.; Kollman, P. A. University of California, San Francisco (USA), 2008.

[35] Wang, J.; Cieplak, P.; Kollman, P. A. How well does a restrained electrostatic potential (RESP) model perform in calculating conformational energies of organic and biological molecules? J. Comput. Chem. 21 (2000) 1049-1074.

[36] Schneider, C.; Sühnel, J. A molecular dynamics simulation of the flavin mononucleotide-RNA aptamer complex. Biopolymers 50 (1999) 287-302.

[37] Morris, G. M.; Goodsell, D. S.; Halliday, R. S.; Huey, R.; Hart, W. E.; Belew, R. K.; Olson, A. J. Automated docking using a Lamarckian genetic algorithm and an empirical binding free energy function, J. Comput. Chem. 19 (1998) 1639-1662.

Graphical abstract

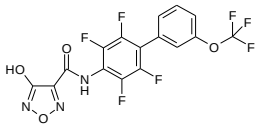

Figure 1

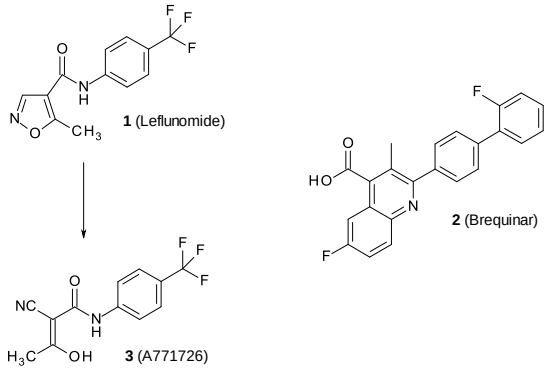

Figure 2

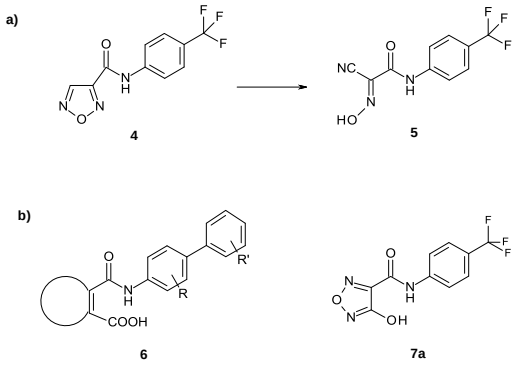

Scheme 1

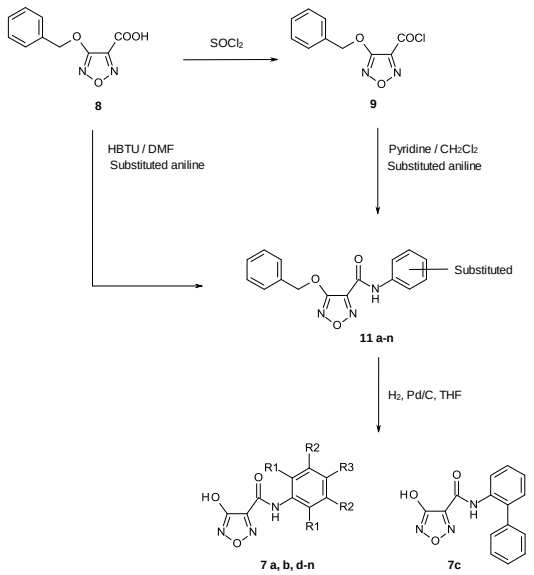

Compd	Substituent		
	R1	R2	R3
a	H	H	CF_3
b	H	H	Ph
d	H	H	4-CF_3Ph
e	H	H	3-CF_3Ph
f	F	H	Ph
g	F	F	Ph
h	F	H	3-CF_3Ph
i	F	H	4-CF_3Ph
l	F	F	4-CF_3Ph
m	F	F	3-CF_3Ph
n	F	F	3-OCF_3Ph

Table 1. Inhibition of rat liver DHODH activity by A771726, Brequinar and compounds **7a-n**

Compd	DHODH inhibition IC_{50} ± SE [μM][a]
A771726	0.020 ± 0.002
Brequinar	0.033 ± 0.004
7a	4.3 ± 0.7
7b	11 ± 1
7c	45 ± 3
7d	49 ± 4
7e	25 ± 2
7f	0.88 ± 0.08
7g	0.066 ± 0.006
7h	0.87 ± 0.11
7i	2.3 ± 0.1
7l	0.49 ± 0.04
7m	0.12 ± 0.02
7n	0.050 ± 0.005

[a] Enzyme activity was measured by DCIP reduction assay and IC_{50} values were calculated with non-linear regression analysis.

Figure 3.

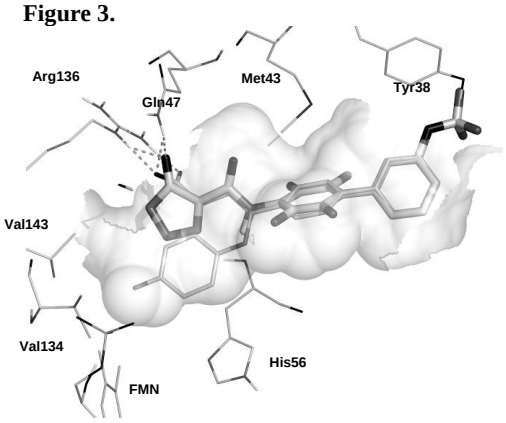

Figure 4.

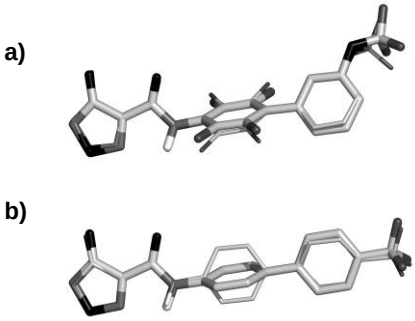

Figure captions

Scheme 1. Synthetic route to compounds object of this work.

Figure 1. Structures of Leflunomide and Brequinar; the most known inhibitors of DHODH.

Figure 2

Figure 3. Docking pose of compound **7n** (thicker sticks) in the human DHODH cavity (PDB ID: 1D3G). The structure of the co-crystallized brequinar analogue is reported for comparison (thinner sticks).

Figure 4. Putative bioactive conformations of compounds **7n** (a) and **7d** (b) (thicker sticks), compared to their respective global minima in solution (thinner sticks).

~~**Table 1.** Inhibition of rat liver DHODH activity by compounds **7a-n**~~